Journal of Structural Geology 26 (2004) 1961–1976

JOURNAL OF STRUCTURAL GEOLOGY

www.elsevier.com/locate/jsg

Analysis of transpressional deformation from geometrical evolution of mesoscopic structures from Phulad shear zone, Rajasthan, India

Sudipta Sengupta*, Subir Kumar Ghosh

Department of Geological Sciences, Jadavpur University, Kolkata 700032, India

Received 10 November 2003; received in revised form 3 May 2004; accepted 3 May 2004

Available online 7 July 2004

Abstract

Transpressional deformation in ductile shear zones may be analyzed by simultaneous wall-parallel simple shear (with strain rate $\gamma^{\bullet} = \gamma^{\bullet}_{xy}$) along with three-dimensional coaxial deformation (with strain rates $\epsilon^{\bullet}_x$, $\epsilon^{\bullet}_y$ and $\epsilon^{\bullet}_z$). Several types of transpression may be distinguished on the basis of relative values of strain-rate ratios $\epsilon^{\bullet}_x/\gamma^{\bullet}$ $(=a)$, $\epsilon^{\bullet}_y/\gamma^{\bullet}$ $(=b)$ and $\epsilon^{\bullet}_z/\gamma^{\bullet}$ $(=c)$. It is possible to identify the nature of transpressional deformation from a detailed analysis of shear zone structures. In the Phulad shear zone of Rajasthan, India, evidence of general flattening, a thrusting sense of shear, occurrence of transport-parallel stretching lineation, frequent occurrence of sheath folds with apical direction parallel to the stretching lineation and occurrence of U-shaped lineation patterns indicate that the deformation was transpressional, with *b*/*a* ratio ranging between -1 and -2. The bulk deformation was not dominated by simple shear, but involved both simple and pure shear, with extrusion along the transport direction much greater than along the vorticity vector. Rotation of long tectonic clasts caused reorientation of monoclinic rolling structures, so that strongly monoclinic structures, with opposite senses of asymmetry in different domains, appear on subhorizontal outcrops parallel to the vorticity vector, although the component of simple shear is zero on these surfaces.

Keywords: Transpression; Ductile shear zones; Stretching lineation; Vorticity; Rolling structures

1. Introduction

Transpressional deformation in a ductile shear zone involves a combination of simultaneous wall-parallel simple shearing and coaxial deformation involving shortening across the shear zone walls. Transpressional deformation may be considered in a variety of increasing complexity. For convenience of description, let us consider a set of coordinate axes, with the *x*- and *z*-axes parallel to the shear zone walls and the *y*-axis normal to the walls. In transpression, there is a shortening across the shear zone walls, i.e. parallel to the *y*-axis. Let the direction of wall-parallel simple shearing be parallel to the *x*-axis. The vorticity vector is parallel to the *z*-coordinate axis (Fig. 1a).

The simplest types of transpression involve homogeneous deformation by a combination of simple and plane strain pure shear. In Ramberg's (1975) model, the *z*-axis, i.e. the direction of the vorticity vector, is a direction of no strain (Fig. 1b); hence, there is an instantaneous extension parallel to *x*-axis, the direction of simple shearing. Sanderson and Marchini (1984) considered another type of plane strain model in which, for the coaxial part of deformation, the *z*-coordinate axis is a direction of extension, and the *x*-axis parallel to the direction of wall-parallel simple shear is a direction of no strain (Fig. 1c). Tikoff and Fossen (1993) have also considered a model of homogeneous transpression in which coaxial straining is combined with three orthogonal simple shears. In another complex model of homogeneous transpression, Jones and Holdsworth (1998) considered a combination of wall-parallel simple shear at an angle to the principal axes of plane strain pure shear, with stretching along the direction of the vorticity vector.

The complexity of transpressional deformation greatly increases when we consider the situation in which there is no free slip at the shear zone boundary, and the material within the shear zone is welded to the rigidly behaving shear zone walls (e.g. Robin and Cruden, 1994; Dutton, 1997). The complexity in this case arises from the fact that the

* Corresponding author. Tel.: +91-33-412-7550; fax: +91-33-414-6375.
E-mail address: jugeossg@iacs.res.in (S. Sengupta).

0191-8141/$ - see front matter © 2004 Elsevier Ltd. All rights reserved.
doi:10.1016/j.jsg.2004.05.002

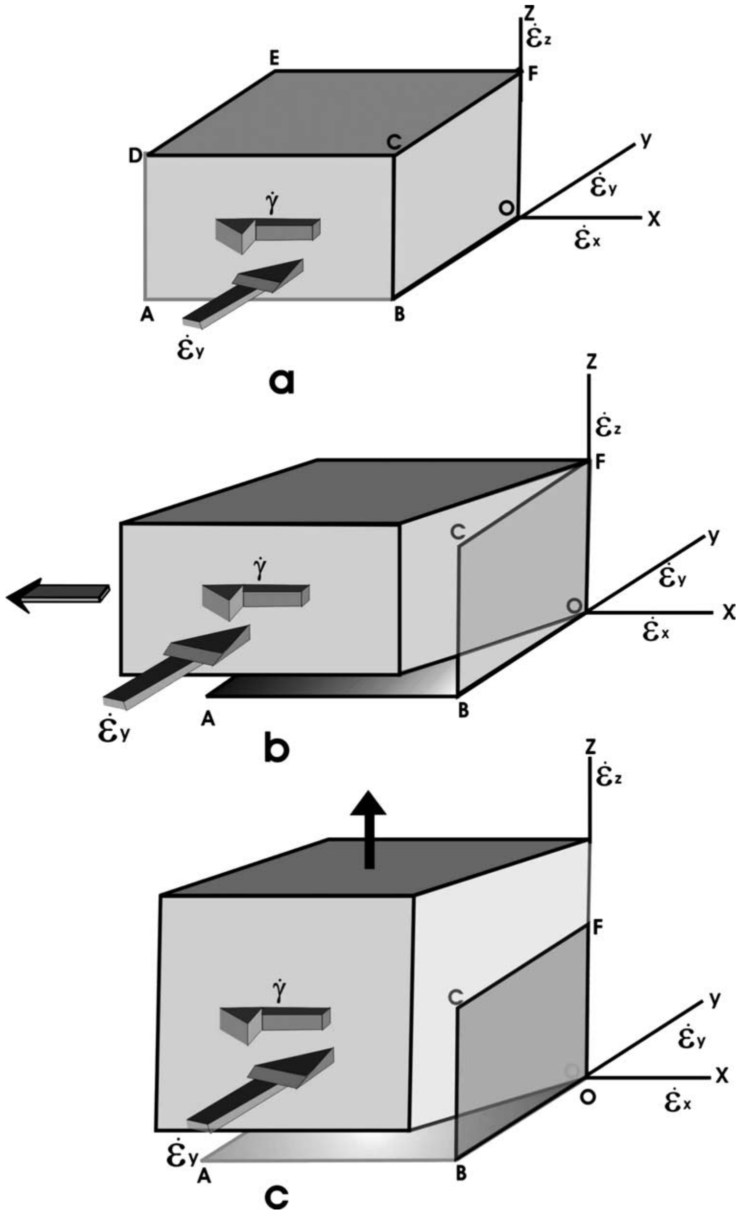

Fig. 1. (a) Orientation of co-ordinate axes, x, y and z with reference to the shear zone walls DCB and EFO. $\gamma^\bullet$ is the rate of wall-parallel simple shear parallel to the x-axis and $\epsilon_x^\bullet$, $\epsilon_y^\bullet$ and $\epsilon_z^\bullet$ are the rates of pure shear. Note that in transpression, $\epsilon_y^\bullet$ causes a shortening across the shear zone. (b) Ramberg's model of plane strain general shear. (c) Sanderson and Marchini's model of plane strain transpression.

nature of instantaneous deformation is heterogeneous and varies from place to place; consequently it also varies for a single material point in the course of progressive deformation.

The orientation of the stretching lineation may show different geometrical relations with respect to the transport direction. In many ductile shear zones, the stretching lineation is parallel to the direction of tectonic transport. On the other hand, stretching lineations perpendicular to the transport direction have been reported from some subvertical transpressional shear zones; many of these have a transcurrent transport direction and a subvertical stretching lineation (e.g. Hudleston et al., 1988; Robin and Cruden, 1994; Greene and Schweickert, 1995). Tikoff and Greene (1997) have described the domainal occurrence of both transport-parallel and transport-normal stretching lineations from the same shear zone. In the model of Robin and Cruden (1994), the orientation of the stretching lineation may show a continuous spatial variation between these two orientations.

With respect to the transport direction, the orientation of the stretching lineation is controlled by the nature of instantaneous deformation as well as by the magnitude of finite deformation. The instantaneous deformation may be regarded as a combination of simple shear (with strain rate $\gamma^\bullet$) and coaxial deformation (with strain rates $\epsilon_x^\bullet$, $\epsilon_y^\bullet$ and $\epsilon_z^\bullet$). The nature of instantaneous transpression would then depend on the ratios between the coaxial strain rates and the rate of simple shear (e.g. Tikoff and Fossen, 1993; Fossen and Tikoff, 1993, 1998; Ghosh, 2001). For high-strain transpressional shear zones in which there is little or no extrusion along the x-coordinate axis (Fig. 1c), a simple shear-dominated deformation produces a stretching lineation parallel to the x-axis, whereas a pure shear-dominated deformation produces a stretching lineation parallel to the vorticity vector or the z-axis. Depending on the ratio of pure and simple shear strain rates, we may have a switching of the direction of maximum stretching from the x- to the z-coordinate axis with progressive deformation. The geometrical relation between the transport direction and the stretching lineation becomes much more complex when there is significant extrusion along the transport direction as well as along the vorticity vector.

2. Orientation of stretching lineation in homogeneous transpression involving simple shear along with three-dimensional coaxial strain

2.1. Homogeneous transpression with simultaneous simple shearing and three-dimensional coaxial strain

Although the model of Robin and Cruden (1994) or, conceivably, a more complex model of transpression involving bulk simple shear and three-dimensional coaxial deformation with no free slip at the boundaries may be considered as realistic, the applicability of such a model of heterogeneous deformation to structures of natural shear zones is restricted (cf. Jones et al., 1997). For the purpose of analyzing structures and the structural history in shear zones in which the foliation and the lineation maintain a more or less uniform orientation, it is advantageous to consider a less complex model of homogeneous transpression (Fig. 2), involving simple shear (with strain rate $\gamma^\bullet = \gamma^\bullet_{xy}$) and three-dimensional coaxial deformation (with strain rates $\epsilon^\bullet_x$, $\epsilon^\bullet_y$ and $\epsilon^\bullet_z$). Among these four parameters, the simple shearing ($\gamma^\bullet$) causes only a plane strain. In transpressional deformation, $\epsilon^\bullet_y$, causing shortening across the shear zone, is always negative. Depending on whether $\epsilon^\bullet_x$ and $\epsilon^\bullet_z$ are both positive, or only one of them is positive and the other is zero or negative, the instantaneous deformation may cause flattening (Fig. 2a), plane strain or constriction (Fig. 2b and c). For our purpose, the relevant parameters are the ratios of strain rates $\epsilon^\bullet_x/\gamma^\bullet$, $\epsilon^\bullet_y/\gamma^\bullet$ and $\epsilon^\bullet_z/\gamma^\bullet$. Let $a = \epsilon^\bullet_x/\gamma^\bullet$, $b = \epsilon^\bullet_y/\gamma^\bullet$, and $c = \epsilon^\bullet_z/\gamma^\bullet$. If there is no volume change, $a + b + c = 0$. With a and b as coordinate axes, the nature of instantaneous deformation can be represented by a point on the ab plane (Ghosh, 2001) and different types of homogeneous transpression can be represented as separate domains (Figs. 3 and 4) on the plane.

The orientation of the stretching lineation with respect to the vorticity vector depends to a large extent on the ratio of b/a. The relative orientation of the stretching lineation also depends on the absolute values of a and b. In simple shear dominated transpression, both $|a|$ and $|b|$ are small; for simple shear, $a = b = 0$. In deformations involving a significant proportion of pure strain, $|a|$ and $|b|$ are large.

2.2. Stretching lineation in different types of transpressional deformation

Depending upon the relative values of a and b we may have in high strain shear zones the following four broad categories of relationships of the stretching lineation, the vorticity vector and the nature of bulk strain (constriction, plane strain or flattening):

(A) Transport-parallel stretching lineation associated with bulk constrictional deformation.
(B) Transport-parallel stretching lineation associated with flattening or plane strain.
(C) Vorticity-parallel stretching lineation associated with flattening.
(D) Vorticity-parallel stretching lineation associated with bulk constrictional deformation.

On the ab plane, the relationship described in (A) is represented in three domains. In domain IX (Figs. 3 and 4), the greatest shortening takes place along the vorticity vector. In other words, the Z-axis of the strain ellipsoid is parallel to the vorticity vector in both low and high strains. Hence the dominant cleavage should be perpendicular to the vorticity vector. In domain VIII, a cleavage parallel to the vorticity vector develops in low to moderate strain. The Y-axis of strain is parallel to the vorticity vector. This cleavage is crenulated. At a high strain the Z-axis becomes parallel to the vorticity, and a new cleavage forms perpendicular to it. In domain VII, the deformation is in the field of constriction, the dominant cleavage is parallel to the vorticity vector but this cleavage is crenulated in the course of the same deformation, with the crenulation axis parallel to the stretching lineation and the crenulation axial plane perpendicular to the vorticity vector. The vorticity vector is parallel to the Y-axis of bulk strain ($Y < 1$). Deformation in all three domains will be characterized by complex folding associated with bulk constriction (Ghosh et al., 1995).

For the relationship described in (B), the cleavage is parallel to the vorticity vector. This type of relationship is shown by the domain VI on the ab plane (Figs. 3 and 4). For this domain $b/a \leq -1.0$ but > -2.0. $b/a = -1.0$ represents plane-strain transpression with extrusion along the transport direction and no strain along the vorticity vector ($c = 0$). This is the type of deformation analyzed by Ramberg (1975) and described as general shear by Simpson and De Paor (1993, 1997). $b/a = -2.0$ refers to a type of transpression in which the rate of extension along the transport direction is equal to that along the vorticity vector ($a = c$). Change in the value of b/a from -1 to -2 means that the ratio of rates of extrusion along the vorticity vector and the transport direction (c/a) increases from 0 to 1.

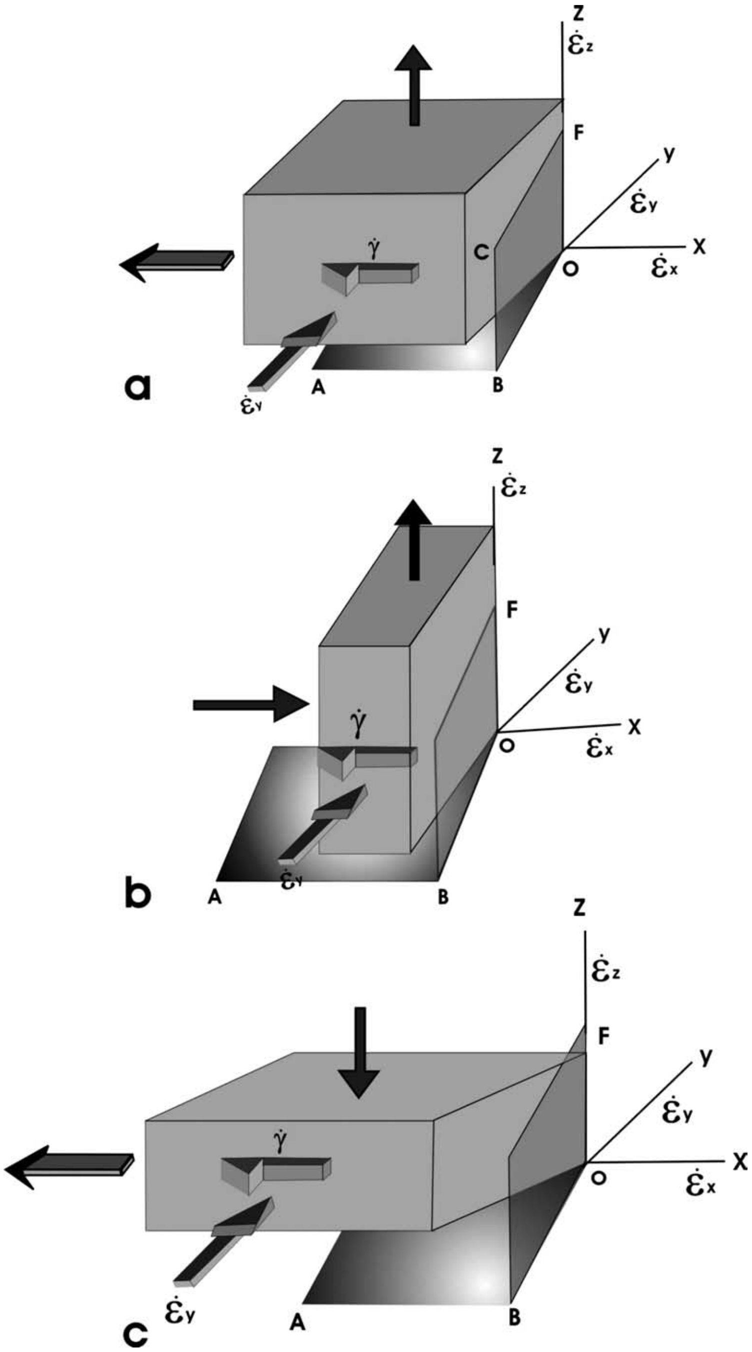

Fig. 2. Model of homogeneous transpression, obtained by simultaneous wall-parallel simple shear and three-dimensional co-axial deformation. (a) Transpressional deformation with extension along both the direction of simple shear (x) and the vorticity vector (z). (b) Transpression with a shortening along the x-axis and an extension along the z-axis. (c) Transpression with extension along the x-axis and shortening along the z-axis.

Within this range of b/a the deformation is of flattening type. The vorticity vector is parallel to the Y-axis of bulk strain ($Y > 1$). There is no switching of the direction of stretching lineation with progressive deformation anywhere within this domain of deformation. In other words, in flattening type of transpressional deformation, in which the rate of extension along the transport direction is greater than along the vorticity vector, the stretching lineation remains perpendicular to the vorticity vector in both simple and pure strain dominated shear zones and in both high and low strains.

The relationship described in (C) is shown by two domains on the ab plane, with b/a ranging between -2.0 and $-\infty$. In domain V, there is a switching of orientation of the stretching lineation with progressive deformation. Initially at low strain, the lineation is perpendicular to the vorticity vector; at high strain it is parallel to the vorticity vector. The deformation remains in the flattening field

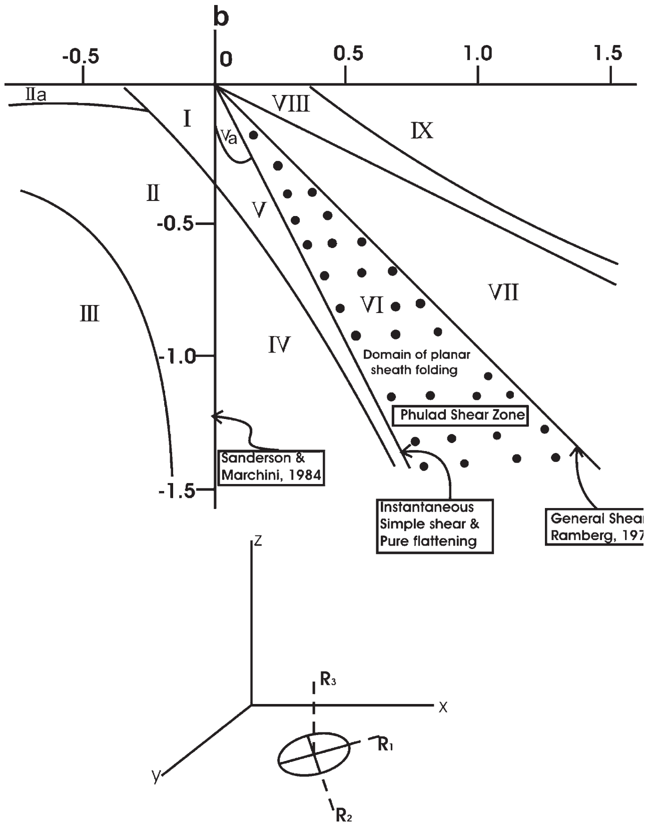

Fig. 3. Domains of different types of transpression on the *ab*-plane, each with its characteristic deformation history. The orientations of principal axes of strain ellipsoid are shown in the lower part. The longer axis of the strain ellipsoid on the *xy*-plane is denoted as R_1, the shorter axis on the plane as R_2 and the principal strain axis parallel to the *z*-coordinate axis is designated as R_3. The nature of deformation depending on the relative magnitude of R_1, R_2 and R_3 are as follows: Domain I: $R_1 > R_3 > 1 > R_2 \rightarrow R_3 > 1 > R_1 > R_2$. Domain II: $R_3 > R_1 > 1 > R_2 \rightarrow R_3 > 1 > R_1 > R_2$. Domain III: $R_3 > 1 > R_1 > R_2$. Domain IV: $R_3 > R_1 > 1 > R_2$. Domain V: $R_1 > R_3 > 1 > R_2 \rightarrow R_3 > R_1 > 1 > R_2$. Domain VI: $R_1 > R_3 > 1 > R_2$. Domain VII: $R_1 > 1 > R_3 > R_2$. Domain VIII: $R_1 > 1 > R_3 > R_2 \rightarrow R_1 > 1 > R_2 > R_3$. Domain IX: $R_1 > 1 > R_2 > R_3$.

throughout the course of deformation. There is a small domain, Va, where the absolute values of both *a* and *b* are small so that the deformation is dominated by simple shear. The stretching lineation in this domain is perpendicular to the vorticity vector and the deformation is of the flattening type as in domain VI. However, in domain V-a, the instantaneous deformation at an advanced stage of deformation shows the maximum *instantaneous* stretching parallel to the vorticity vector. In domain IV, the stretching lineation is parallel to the vorticity in both high and low strains. The rate of extension along the vorticity vector is greater than along the transport direction ($a \leq c$). It may be noted that $b/a = -\propto$, i.e. the line $a = 0$, $b < 0$, in Fig. 3, represents the type of transpression considered by Sanderson and Marchini (1984).

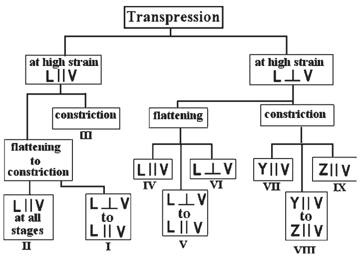

Fig. 4. Subdivision of different types of transpressional deformation based on the stretching lineation (*L*) with respect to the vorticity vector (*V*) and the nature of bulk deformation.

The relationship described in (D) is shown by domains I–III on the *ab* plane (Fig. 3). In domain III the bulk deformation is constrictional in both low and high strains. The cleavage is crenulated in all stages of deformation, with the crenulation axis parallel to the vorticity vector and the stretching lineation. In domain II, the bulk deformation is of flattening type in the initial stages, but at high strain the bulk deformation is of constrictional type. Thus, there is a shortening both across the shear zone and along the transport direction. Hence, the vorticity-parallel cleavage should be crenulated at an advanced stage of deformation. In domain I the bulk deformation in the initial stages is of the flattening type and the stretching lineation is perpendicular to the vorticity vector. With progressive deformation the stretching lineation switches to become parallel to the vorticity vector while the deformation remains in the field of flattening. However, the deformation enters into the field of constriction at a very advanced stage.

A greater insight into the nature of the transpressional deformation is obtained when, along with the orientation of the stretching lineation, we also consider the evolution of other structural elements, especially the history of shear zone folding, development of shear zone cleavage and the geometry of rolling structures around clasts.

3. Contemporaneous folding history in transpressional shear zones

Foliation in ductile shear zones often shows contemporaneous folding (i.e. folding during the course of ductile shearing). The shear-related folds generally initiate at a right angle to the direction of the component of simple shear (e.g. Bryant and Reed, 1969; Sanderson, 1973; Escher and Watterson, 1974; Carreras et al., 1977; Rhodes and Gayer, 1977; Bell, 1978; Quinquis et al., 1978; Minnigh, 1979; Cobbold and Quinquis, 1980; Ramsay, 1980; Ghosh and Sengupta, 1984, 1987, 1990; Mies, 1991; Alsop, 1992; Crispini and Capponi, 1997; Sengupta and Ghosh, 1997; Alsop and Holdsworth, 1999; Ghosh et al., 1999). The course of progressive evolution of the folds would, however, depend on the type of transpressional deformation.

In transpression involving an instantaneous shortening along the vorticity vector, i.e. for domains of transpression (Fig. 3) in which b/a lies between 0 and -1, the bulk deformation will be constrictional. Folds initiating parallel to the vorticity vector will be deformed by hinge-parallel shortening. The resulting structure is likely to show domes and basins along with nonplane, noncylindrical folds of diverse orientations (cf. Ghosh et al., 1995).

If the bulk deformation is of the flattening or plane strain type (b/a ranging between -1 and $-\infty$), we have two situations depending on whether the rate of extension parallel to the direction of simple shear is greater or less than the extension rate along the vorticity vector ($a>c$ or $a<c$). Note that, since $a+b+c=0$, $a=c$ means that $b/a=-2$. If $a>c$, ($b/a\leq -1$ but >-2), the folds initiating parallel to the vorticity vector will be at a right angle to the direction of stretching. Since this orientation of the fold hinge or of any other linear element is unstable, a slight deviation from exact orthogonality will cause it to rotate towards the stretching direction. In high strain zones the hinge lines will rotate through a large angle and tend to become parallel to the transport direction. If the hinge lines have an initial curvature, the curvature will increase with progressive deformation and sheath folds with planar axial surfaces will be produced at high strain.

If both a and c are positive (Fig. 3), but $a<c$, as in domain IV, the hinge lines of folds initiating parallel to the vorticity vector and to the stretching lineation do not undergo rotation of the hinge lines. Contemporaneous sheath folds cannot develop in such transpressional shear zones. The rotation history of the folds will be somewhat more complex for domain V, in which folds initiating parallel to the vorticity vector will first rotate towards the transport direction, but at an advanced stage of deformation the folds will rotate back towards the vorticity vector. Sheath folds are unlikely to develop under these conditions.

In transpressional shear zones in which there is an instantaneous shortening in the direction of transport, ($a<0$, $b<0$ and $b/a>0$), the bulk deformation will be constrictional. The fold axis will always be parallel to the stretching lineation and the vorticity vector. In high strain shear zones the cleavage will be coaxially crenulated. There will be no rotation of fold hinge lines.

From the foregoing analysis it is evident that rotation of fold hinge lines and development of planar sheath folds (Ghosh et al., 1999) is possible only in those transpressional shear zones in which the stretching lineation is at a right angle to the vorticity vector and the bulk deformation is of the flattening (or plane strain) type, with the rate of stretching along the transport direction distinctly greater than along the vorticity vector (Fig. 3).

4. Nature of transpressional deformation in Phulad shear zone, Rajasthan, India

The Phulad shear zone of the Delhi mobile belt of western India (Ghosh et al., 1999) is marked by a zone of mylonite with a more or less uniform orientation of the foliation and lineation. The average orientation of the foliation is 035/70E, and the lineation plunges essentially down the dip. The lineation is a stretching lineation marked by strongly elongated grains of quartz.

Several generations of folds on the mylonitic foliation developed in the course of ductile shearing. The earliest of these folds occur as reclined folds with down-dip plunge of the hinge line and with axial surfaces parallel to the shear zone.

In the Phulad shear zone, the orientations of the principal strain axes can be determined. However, in the absence of suitable strain gauges, the magnitudes of the components of principal strain are unknown. A qualitative assessment of the nature of deformation can, nevertheless, be made from an analysis of patterns of deformed lineations, the rotation history of folds and of other linear structures, and from the geometry of pressure shadows (or tails) associated with porphyroclasts.

The mylonitic lineation is often deformed by the shear zone folds. A characteristic pattern of deformed lineations is the U-pattern (Ghosh and Chatterjee, 1985; Ghosh and Sengupta, 1984, 1987, 1990; Sengupta and Ghosh, 1997; Ghosh et al., 1999). In the U-pattern (Fig. 5a), the lineation appears in a strongly curved form when the folded surface is unrolled. The U-pattern may be symmetric or asymmetric (Fig. 5b and c). On the unrolled form surface of the fold, the point of maximum curvature of a symmetrical pattern of deformed lineation lies on the position of the hinge line of the fold. In an asymmetrical pattern the point of maximum curvature of the lineation lies on one side of the hinge line. An analysis of the U-patterns of lineation (Ghosh and Chatterjee, 1985; Ghosh and Sengupta, 1987, 1990) shows

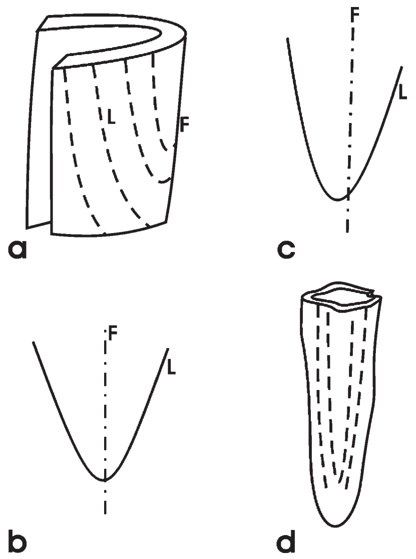

Fig. 5. (a) U-pattern of lineation (L) over a fold produced by the combined process of buckling and flattening. (b) When the fold in (a) is unrolled the lineation shows a U-pattern symmetrical about the fold hinge. (c) When the fold in (a) is unrolled the lineation may show a U-pattern whose point of maximum curvature does not lie on the fold hinge. This is an asymmetrical U-pattern. (d) Sheath fold with oval outcrop and with curved hinge line greatly drawn out in the down-dip direction.

that the folds that developed in the course of ductile shearing were initially subhorizontal; their hinge lines were rotated towards the down-dip direction of stretching. Analysis of deformed lineations (Ghosh et al., 1999) also indicate that simple shear dominated deformation cannot produce symmetrical U-patterns of lineations. Since symmetrical patterns are common in the Phulad shear zone, it may be concluded that the ratio of pure shear to simple shear was significantly large. The last generation of folds is the least rotated, and is subhorizontal or gently pitching. These are strongly asymmetrical folds and their sense of asymmetry always indicates a thrusting sense of movement.

The Phulad shear zone shows profuse development of sheath folds from the scale of hand specimens to outcrop scale. Unlike many other areas of sheath folding, the three-dimensional forms of the sheath folds are exposed in many places in the Phulad shear zone (Figs. 6b and 10c). The sheath folds, with their hairpin bends of the hinge lines, are greatly drawn out in the down-dip direction (Figs. 5d and 9b and c). Flattened oval outcrops of sheath folds are plentiful. Sections parallel to the axial planes of sheath folds show strongly curved intersection lineations (Fig. 6c and d). The geometry of the sheath folds also indicates that the direction of maximum stretching in the shear zone is essentially orthogonal to the vorticity vector.

Pressure shadows associated with porphyroclasts are relatively uncommon in the Phulad shear zone. However, pressure shadows associated with some of the near spherical porphyroclasts occur in both *XZ* and *YZ* sections, indicating thereby that there was some extension along the *Y*-axis of the strain ellipsoid, i.e. along the vorticity vector.

Deformation in the Phulad shear zone is, thus, transpressional ($b<0$) and of the flattening type, with a subhorizontal vorticity vector orthogonal to a thrusting sense of shear. In Fig. 3 it belongs to the domain of transpression with $b/a < -1$ and > -2, with positive values of both a and c and with $a > c$. Since rotation of fold hinge lines was very common, and the hinge lines of earlier generations of contemporary folds have rotated through large angles to become essentially parallel to the stretching lineation, it is likely that stretching parallel to the transport direction was very much in excess of the stretching along the vorticity vector, i.e. $a \gg c$. In other words, it is likely that the value of b/a was much closer to -1 than to -2. As mentioned above, the frequent occurrence of symmetrical U-patterns of lineations indicate that the ratio of pure shear to simple shear was fairly large. In other words, the absolute values of $|a|$ and $|b|$ are likely to have been moderately large.

5. Occurrence of resistant remnants

The mylonites of the Phulad shear zone are in most parts very fine-grained orthomylonites and ultramylonites. However, the rocks also contain large tectonic clasts; the largest of them is about a metre long. The tectonic clasts belong to several categories, i.e. boudins, detached fold hinges, isolated bodies of quartzofeldspathic pegmatite and porphyroclasts of feldspar.

There are different transitional stages of change from large clasts of pegmatite to single-crystal porphyroclasts. The larger clasts, up to a metre long, are lenticular bodies parallel to the mylonitic foliation (Fig. 6e and f). These have strongly sheared borders and long tails extending into the foliated matrix. The pegmatitic clasts and their tails are composed of both quartz and feldspar. As the tails thin out, they become orthomylonitic and contain isolated porphyroclasts of feldspar in a fine-grained quartzofeldspathic matrix. The main body of the clast is subdivided into smaller elongate quartzofeldspathic clasts bounded by narrow shear zones. These internal shear zones show a well-developed fine mylonitic layering and they contain smaller quartzofeldspathic clasts and single crystal porphyroclasts of feldspar. Within the internal shear zones, the originally coarse crystals of quartz and feldspar have recrystallized to fine grains, and the recrystallized domains have been drawn out to produce alternate quartz- and feldspar-rich bands. Progressive grain size reduction and drawing out of the recrystallized product of very coarse crystals of feldspar have also produced a fine banding of slightly different grain sizes of feldspar.

In large thin sections we often see successive stages of subdivision of a single megacryst of feldspar into smaller and smaller units (Fig. 7) until an orthomylonitic texture is produced with isolated small and medium sized (millimetric) porphyroclasts surrounded by a recrystallized matrix. In an early stage a single megacryst is subdivided into smaller porphyroclasts with irregular grain borders. The matrix itself may show various intensities of foliation development. In many cases, the successive stages of shrinking in size, say, from a centimetre-scale porphyroclast to a set of sub-millimetre-scale porphyroclasts do not always involve the development of a core-and-mantle structure. The recrystallized product surrounding each individual porphyroclast is well foliated and is indistinguishable from the matrix (Fig. 7). Indeed, in the Phulad shear zone, mantle-free porphyroclasts with a strongly foliated matrix are more common than porphyroclasts with an apron of unfoliated recrystallized product or a foliated tail that can be distinguished from the matrix (Fig. 8).

Large outcrop-scale clasts of pegmatite are absent in the major part of the Phulad shear zone. There are, however, in many places, in the scale of hand specimen, isolated clasts with smooth elliptical cross-sections ranging in size from a few centimetres to a few decimetres. Many of these tectonic clasts are much larger in one direction. The long axis of the clasts may occur at different angles with the down-dip stretching lineation, although most of them are subparallel to it.

The very fine-grained mylonites of the Phulad shear zone have undergone extreme stretching (Ghosh et al., 1999), and the uniform orientation of the mylonitic

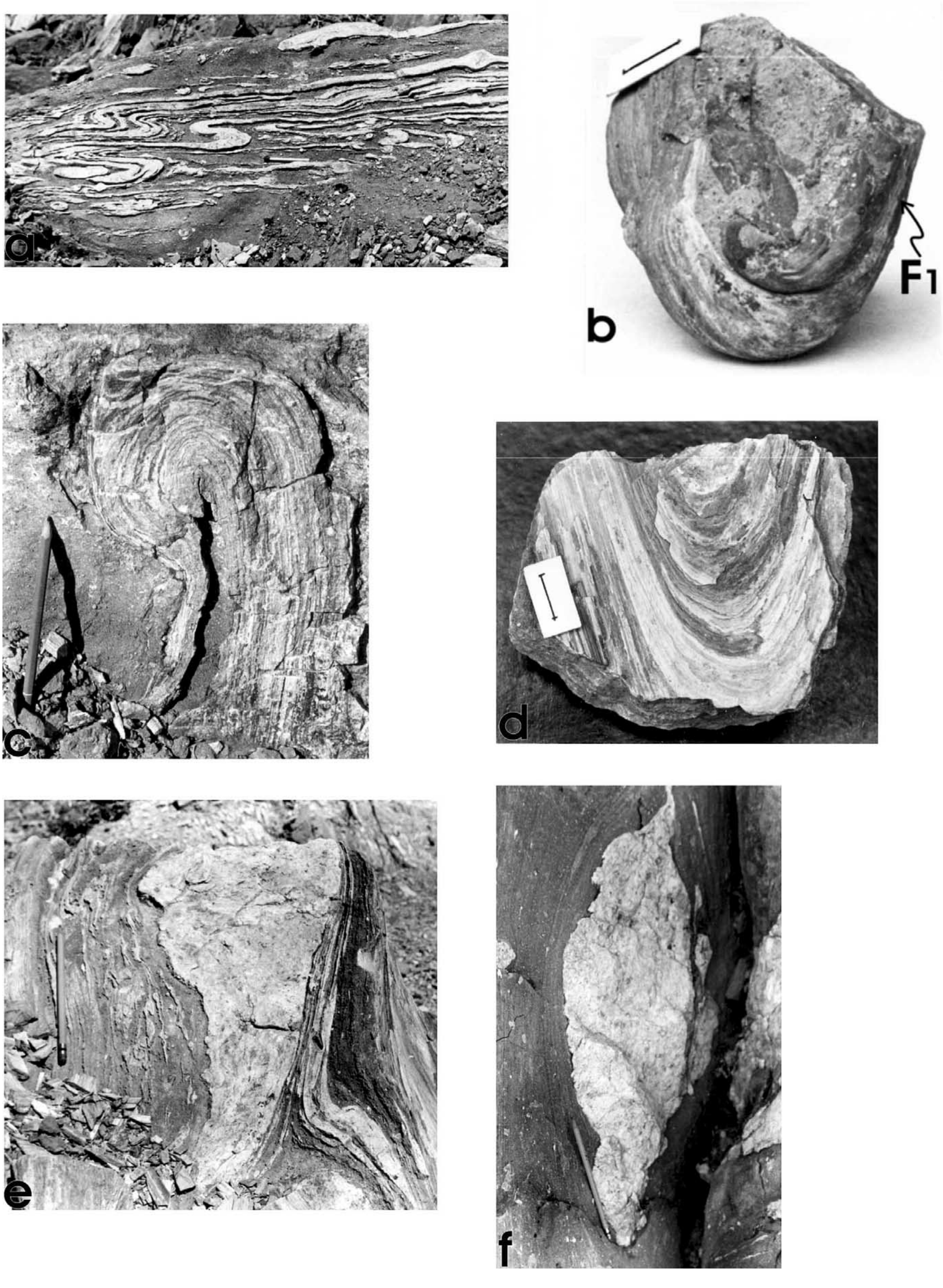
a
b
F_1
c
d
e
f

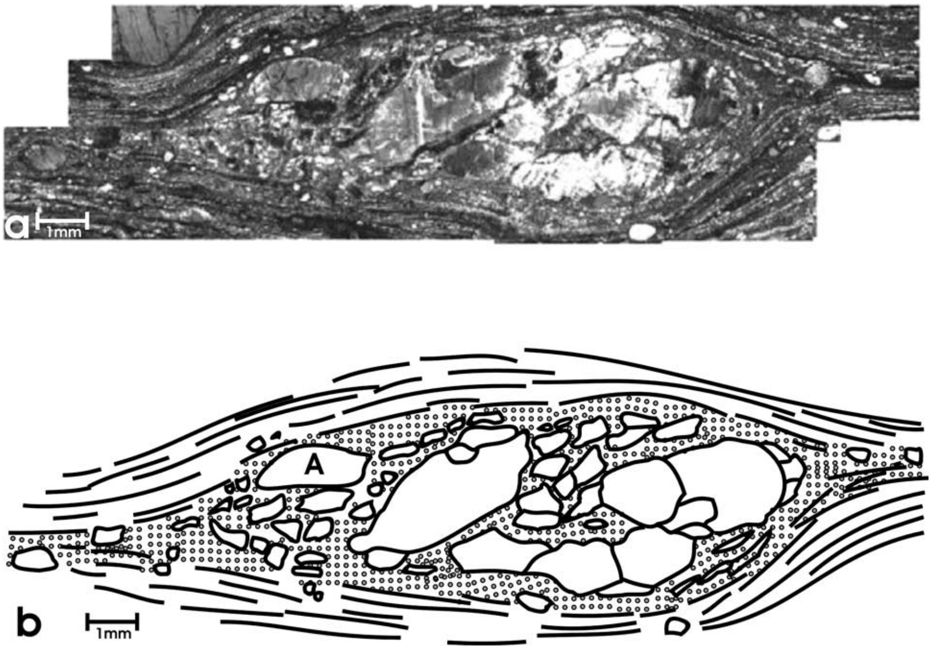

Fig. 7. Photomicrograph (a) and sketch (b) showing subdivision of a megacryst of microcline. The large megacryst is separated into smaller strained porphyroclasts with intervening areas occupied by very fine recrystallized grains. In the central part there is no foliation in the recrystallized material. Towards the margin the recrystallized material is strongly foliated and has developed a banding marked by fine bands of slightly different grain size and elongated small remnant grains. The tails on either side extend into the matrix and are strongly foliated. The porphyroclast A, for example, obtained from the megacryst does not have a clearly discernible mantle attached to it. The recrystallized material at the contact is well foliated.

foliation is essentially parallel to the shear zone boundaries. The tectonic clasts preserve structures produced at different stages of ductile shearing. The incipient foliation that develops even in the weakly sheared portions of these resistant remnants is at a low angle to or is nearly parallel to the general orientation of the shear zone foliation outside the clasts. This low-angle (a few degrees) orientation of the newly produced foliation confirms that the bulk deformation in the shear zone was transpressional, with both simple shearing and coaxial deformation. If the deformation was simple-shear dominated, the weakly sheared domains would have shown a foliation close to 45°.

Apart from clasts that are remnants of pegmatitic bodies, there are long tectonic clasts of boudins and detached fold hinges of competent layers and multilayers. The longest axis of both these types of clasts is parallel to the mylonitic foliation. The long tectonic clasts represented by detached fold hinges are isolated cylindrical bodies with nearly circular or elliptical cross-sections. In cross-section, the internal foliation within these bodies is isoclinally folded, often with a swirling pattern produced by coaxial folding and sheath folding (Fig. 9). Indeed some of these strongly linear bodies are extremely stretched detached sheath folds. The internal foliation ends discordantly with the clast-boundary and with the rolling structure of the outer foliation around it. The cross-sections of these cylindrical bodies are a few centimetres in diameter whereas the clasts are a few tens of centimetres long in the direction of the cylinder axis. Although the axes of these long cylindrical clasts may lie at different orientations on the foliation surface, the majority of them are parallel to the down-dip stretching lineation.

6. Reorientation of monoclinic structures

6.1. Reorientation of asymmetric folds

Monoclinic structures such as asymmetric folds and rolling structures around rigidly rotating clasts will be ordinarily visible in sections parallel to the *xy*-coordinate plane, i.e. in a plane perpendicular to the vorticity vector; monoclinic structures will be absent in the *yz*-coordinate plane parallel to the vorticity vector. This general scenario will be considerably modified when there is a rotation of the hinge lines of shear zone folds and of the major axis of long

Fig. 6. (a) Asymmetrical folds on horizontal section of Phulad shear zone. Scale shown by matchstick at the centre. (b) Three-dimensional form of a planar sheath fold. The hinge line F_1 is curved to a hairpin bend. The intersection lineation is also similarly bent. On the upper surface the outcrop of the sheath fold is oval. In spite of the isoclinally bending of the hinge line, the axial surfaces remain planar. Scale bar 1 cm. (c) and (d) Section parallel to the axial surface of sheath folds. The photographs show the hairpin bend of the intersection lineation. Scale bar in (d) is 1 cm. (e) and (f) Large lenticular pegmatite clast in dip sections of mylonites.

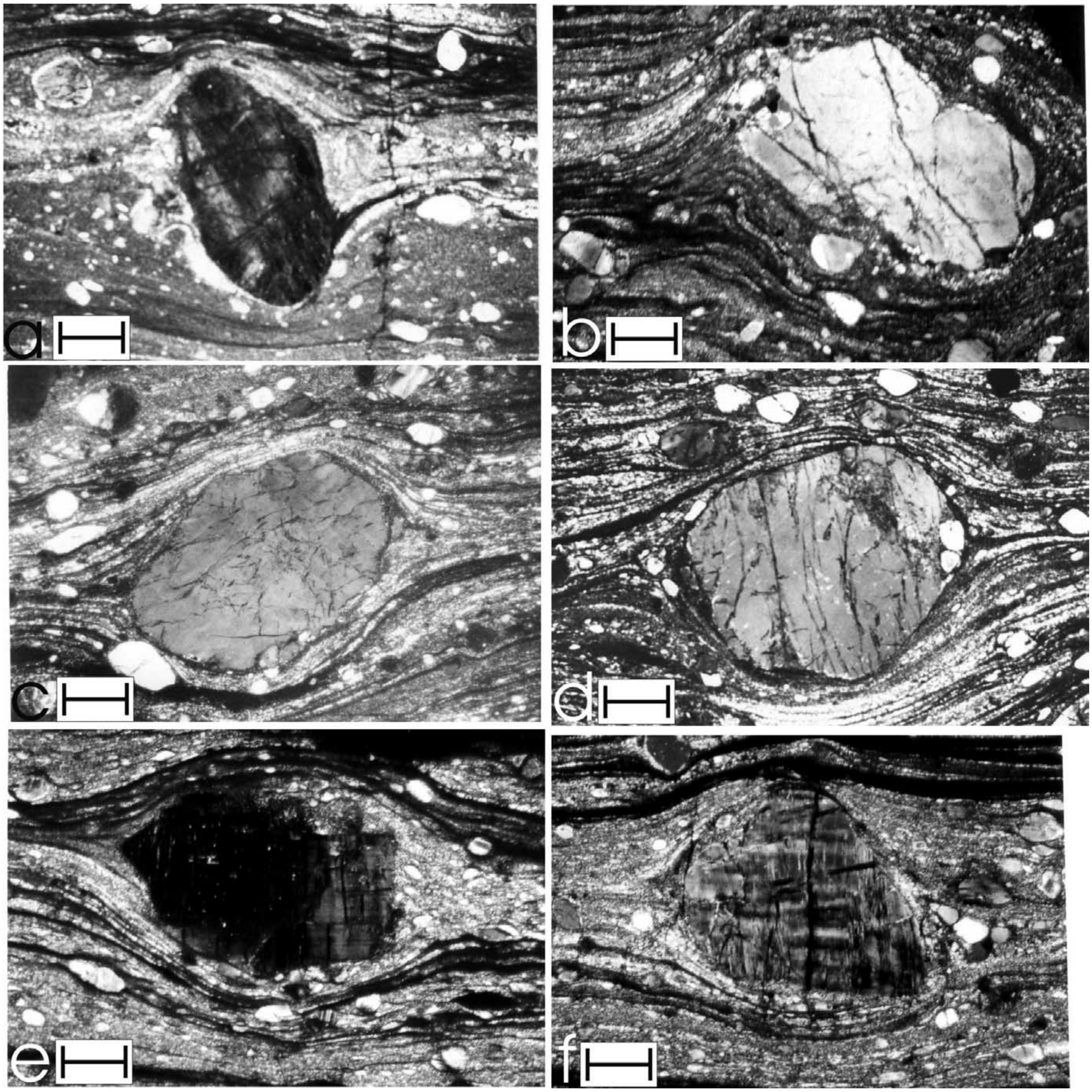

Fig. 8. Photomicrograph of feldspar porphyroclasts of mylonites of Phulad shear zone. (a) δ-Type feldspar megacryst with moderate rotation. (b)–(d) Shows second type of rolling structures around porphyroclast without clearly recognizable mantle around them. (b) and (c) Weakly asymmetric distortion of foliation around the megacrysts. (d) Nearly symmetric swerving of foliation around the feldspar megacryst. (e) Porphyroclast of microcline with a tapering mantle on the right side and a much shorter mantle on the left hand side. Note incipient development of foliation of mantle in the right hand side. (f) Porphyroclast with weak drag pattern of foliation around it. Scale bar 0.03 mm.

tectonic clasts (Ghosh et al., 2003). In the Phulad shear zone, the asymmetric folds were initiated parallel to the subhorizontal vorticity vector. In vertical dip-sections at a right angle to the vorticity vector, the sense of asymmetry of the least rotated subhorizontal folds always corresponds to a thrusting sense of shear. When the hinge lines rotate towards the down-dip direction of stretching, the asymmetric F_1 folds also appear on the horizontal surface. The sense of asymmetry will depend on whether the F_1 hinge line is rotated in a clockwise (Fig. 10b) or anticlockwise (Fig. 10a) sense. When the folds are rotated to become reclined, the asymmetry of the folds appears on their profile plane in horizontal outcrop faces (Fig. 6a), although, being parallel to the vorticity vector, the magnitude of shear on these planes is zero. Again, depending on their initial orientation, the sense of rotation of the hinge lines was opposite in

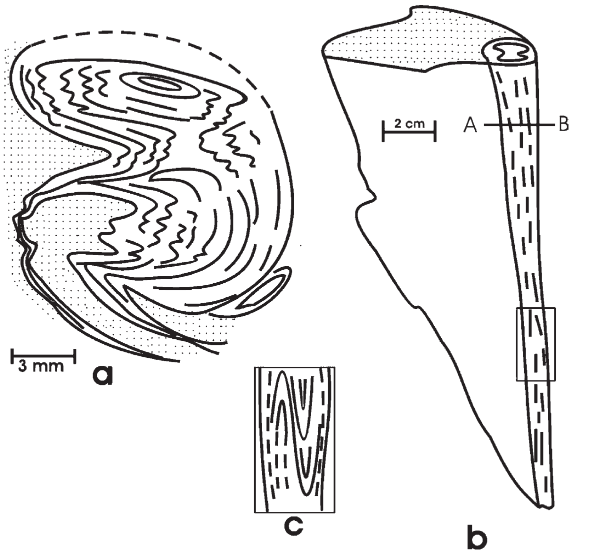

Fig. 9. (a) Swirling pattern of foliation in a cross-section of a detached sheath fold. (b) Three-dimensional form of the same sheath fold with closed horizontal outcrops and strongly elongated hinge lines in the down-dip direction. The pattern shown in (a) is from a section along AB. (c) Details of the longitudinal section for the rectangular domain shown in (b). The detailed structure shows strongly curved upward and downward closing intersection lineation, indicating presence of smaller sheath folds.

different domains (Fig. 10a and b). Consequently, both S- and Z-folds of a layer frequently appear along the same strike line on horizontal outcrops (cf. Hazra, 1997). In horizontal sections, there is a similar change in the sense of asymmetry of the smaller asymmetric folds on the same limb of a relatively larger sheath fold (Fig. 10c). Hence, these rotated minor folds appear to give both dextral and sinistral senses of shear on the horizontal outcrop face even though the true magnitude of shear is zero on this face.

The nature of asymmetry of the F_1 folds deformed by F_2 in a type 2 interference pattern (Ramsay, 1967) will depend upon the nature of deformation during F_2 folding. If the F_1 hinge lines are refolded by F_2 flexure folding without significantly large homogeneous strain, the angle between F_1 and F_2 will remain constant all over the fold (Fig. 11a). In such a case the sense of asymmetry of the F_1 folds remain the same on both limbs of F_2 in its profile plane (Fig. 11c). This is because a single F_1 hinge line deformed by F_2 cannot intercept the F_2 profile plane in more than one point. On the other hand if the nature of deformation during F_2 is such that external rotation around the F_2 hinge is accompanied by a very large stretching parallel to the F_2 axis (Ghosh and Chatterjee, 1985; Ghosh and Sengupta, 1987; 1990), the F_1 hinge is deformed into a U-shaped pattern (Fig. 11b and d)

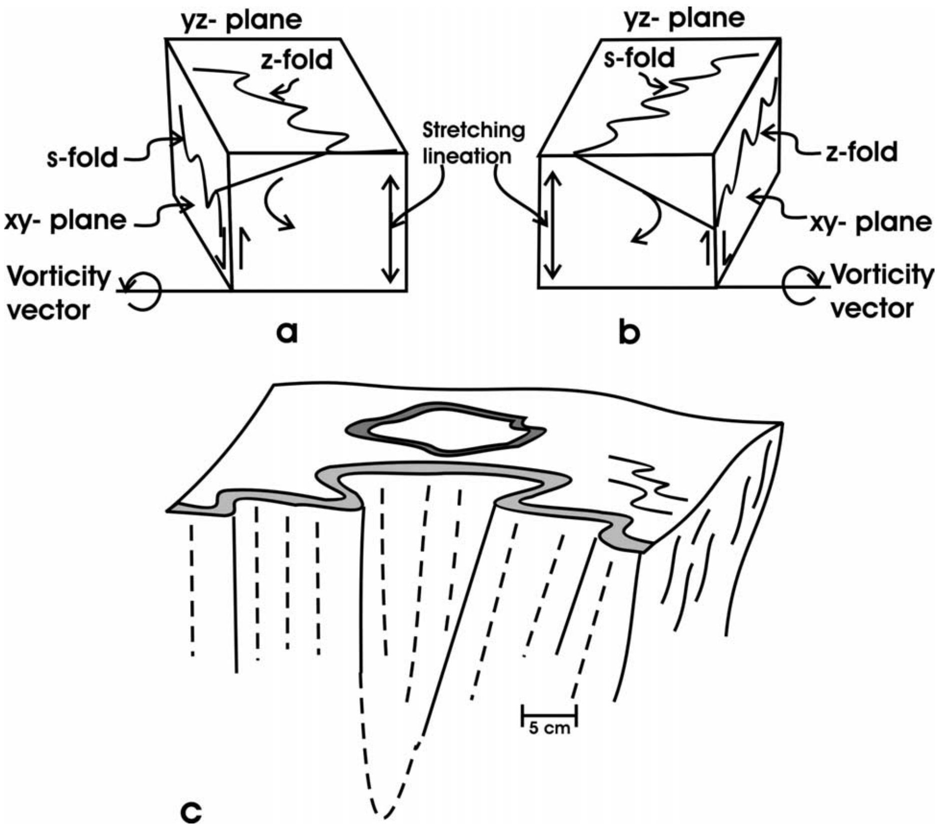

Fig. 10. (a) Asymmetric folds produced by a thrusting sense of shear with S-folds on the left-hand side dip section. The folds appear as Z-folds on the horizontal surface. In response to down-dip stretching the hinge line rotate in a counter-clockwise sense within the shear zone foliation. (b) Asymmetric Z-folds on the right hand side dip-section. The folds appear as S-folds on the horizontal surface. With progressive deformation, the hinge line rotates in a clockwise sense. (c) Mesoscopic sheath folds in the Phulad shear zone. Because of the hairpin bend of the hinge line both S- and Z- folds appear on the same limb of the sheath fold on horizontal section. Only short cylindrical segments of the folds are shown.

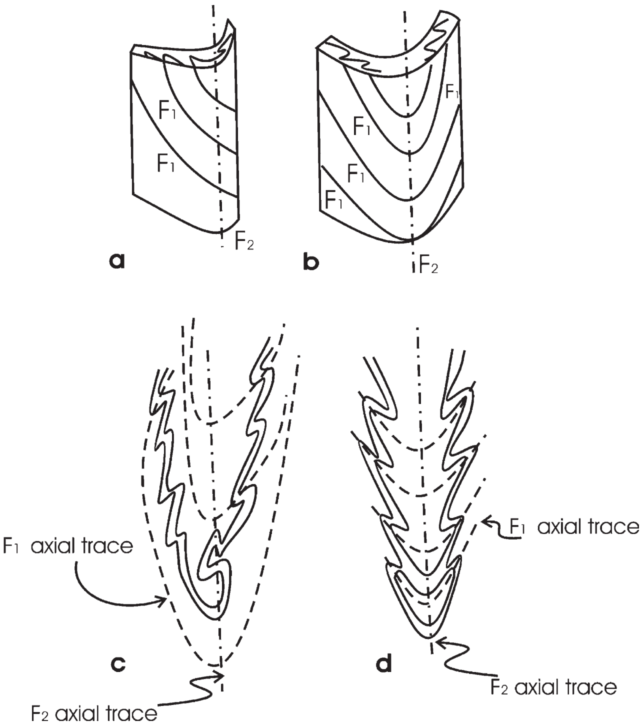

Fig. 11. (a) Small asymmetric F_1 refolded by larger F_2 with the angle between the F_1 and F_2 hinge lines changing all over the F_2. In a section at an angle to F_2 axis, the F_1 folds have the same sense of asymmetry (i.e. S-folds) of both limbs of F_2 as in (c). (b) Shows the F_1 hinge lines deformed to a U-pattern over F_2. A single F_1 hinge line intercepts the F_2 profile plane in two points. In a section at an angle to F_2, the asymmetric F_1 folds appear as S-folds on one limb and Z-folds on the other limb as in (d).

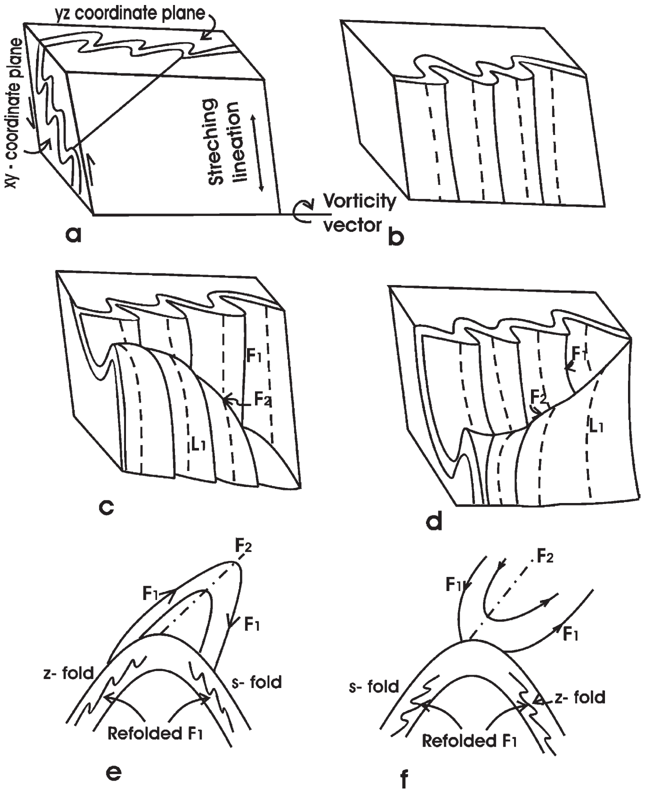

Fig. 12. The asymmetry of the minor folds in a ductile shear should be used with some caution. The complexity that can arise is illustrated in (a)–(f). The F_1 folds produced by ductile shearing, as in (a), are rotated to become reclined, as in (b). The F_1 hinge lines are then refolded by F_2. In (c) the F_2 hinge line forms an upward closing structure. The hinge lines of F_1 and the stretching lineation are deformed in a U-shaped pattern over the F_2 hinges as in (e). F_2 in this case rotated in a clockwise direction. On the profile of F_2 in (e), the refolded F_1 appear as Z-folds on the left limb and S-folds on the right limb as in a congruous antiform. In (d) the F_1 hinge line is a downward closing structure, the major part of the F_2 hinge is rotated in response to down-dip stretching in an anticlockwise sense. The U-shaped F_1 hinges over the antiformal F_2 fold are as in (f). On the profile plane of F_2, the S- and Z-shaped folds are similar to incongruous minor folds with respect to a larger F_2 fold.

so that a deformed F_1 hinge line can meet the F_2 profile plane in more than one point. A Z-shaped F_1 fold on one limb of an F_2 fold appears as an S-shaped F_1 fold on the other limb of F_2 in its profile plane.

The asymmetry of the shear zone minor folds should be interpreted with some caution. Complications arise when, with progressive ductile shearing, the F_1 folds are refolded by F_2 (Fig. 12c and d). With continued shearing the F_2 hinge lines themselves rotate towards the down-dip direction either in a clockwise (Fig. 12c) or an anticlockwise (Fig. 12d) sense. The rotated F_1 folds on the two limbs of F_2 with opposite senses of asymmetry are either similar to the congruous asymmetry of minor folds over a larger F_2 fold (Fig. 12e) or are incongruous on the two limbs of F_2 (Fig. 12f). The process is described in (a)–(f) of Fig. 12. Thus, Fig. 12a shows an initial F_1 fold occurring at an angle to the direction of maximum stretching. The figure shows a thrusting sense of shear and S-folds on the left-hand face of the dip-section (evidently the right-hand dip-section would show Z-folds). Fig. 12b shows the stage in which the F_1 fold hinges have rotated to become parallel to the down-dip stretching lineation. In Fig. 12c, the F_1 hinge lines are refolded by F_2 and the F_2 hinge lines are rotated by a clockwise movement as we look across the strike. The hinge lines of F_1 have been deformed to a U-shaped pattern. On the profile plane of F_2 (Fig. 12e), Z-folds of F_1 are seen on the left limb of the antiformal F_2 fold and S-folds are seen on the right limb. This contrast of fold asymmetry is what we expect in minor folds, which are congruous to the larger fold. On the other hand if the F_2 hinge lines are rotated in an anticlockwise manner as in Fig. 12d, the profile of F_2 (Fig. 12f) will show S-folds on the left limb of antiformal F_2 and Z-folds on the right limb. This configuration is similar to incongruous minor folds.

6.2. Geometry of rolling structures

Van Den Driessche and Brun (1987) have recognized two end members of rolling structures In porphyroclasts in which a tail forms by drawing out of the mantle material, the rolling structure is produced by the deformation of the tail. The second type, without a recognizable mantle, results from deformation of preexisting planar structures around rotating objects (e.g. Ghosh, 1975, 1977; Ghosh and Ramberg, 1976). Both types of rolling structures occur in the Phulad shear zone.

Rolling structures of both types show a wide range of the degree of asymmetry. The strongest asymmetry was found associated with moderately large quartzofeldspathic clasts in the scale of a hand specimen (from a few centimetres to a decimetre). The mylonitic foliation in its neighbourhood is asymmetrically deformed, with the embaying fold forming an isoclinal overturned structure, and with the foliation bending through 180° (Fig. 13). Strongly asymmetric rolling structures are also found around large (a few millimetres to a centimetre) single-crystal porphyroclasts of feldspar (Fig. 14a–d). Monoclinic δ types of mantled porphyroclasts (Passchier and Simpson, 1986; Passchier, 1987) with a moderate degree of asymmetry are frequently found in thin sections (Fig. 8a).

The transitional stages of change from a large tectonic clast to a smaller polycrystalline clast or a single-crystal porphyroclast shows that, in the initial stage, the clasts are angular; they attain smooth borders when the clast–matrix ratio in the rock has become small. Along with this process of change in the shape and size of the clast, the recrystallized product becomes increasingly better foliated. Each isolated clast with smooth border and relatively small aspect ratio is likely to have started with a mantle of recrystallized fine-grained material. The second type of rolling structures (without a mantle) forms when the aprons of syntectonically recrystallized materials are so deformed and foliated that they become indistinguishable from the foliated matrix.

Strongly asymmetric structures are generally found in the second type of rolling structures of Van Den Driessche and

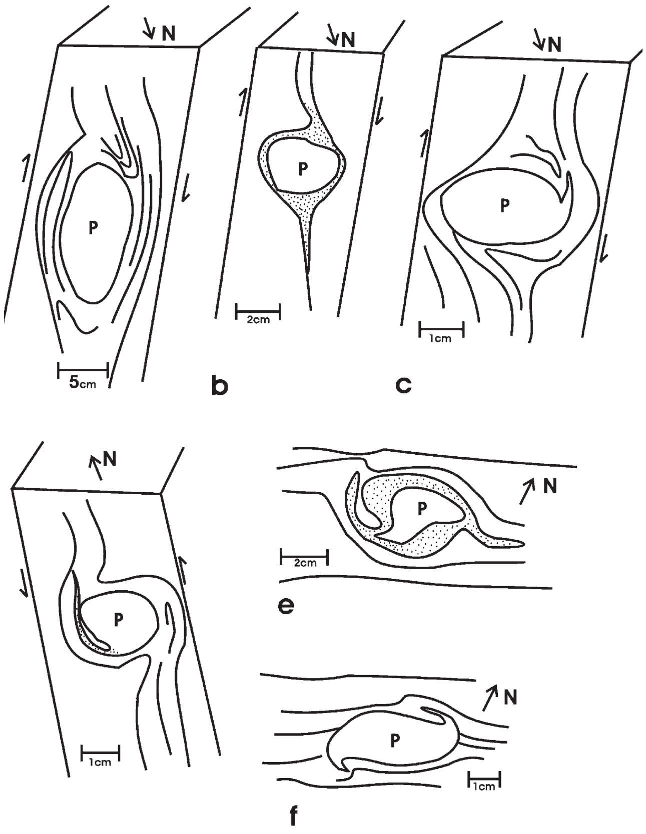

Fig. 14. (a)–(c) Porphyroclasts of feldspar seen in NE facing dip-sections of the Phulad shear zone showing clockwise rotation in conformity with a thrusting movement. The rolling structures in (a) and (c) are shown by deformed matrix in the foliation; in (b) we can see the asymmetric tail in the mantle (dotted). (d) Counter-clockwise rotation of porphyroclast in SW facing dip-section. (e) Apparent sinistral asymmetry of porphyroclast mantle system in horizontal section. (f) Apparent dextral rotation of porphyroclast in horizontal section. P—porphyroclast.

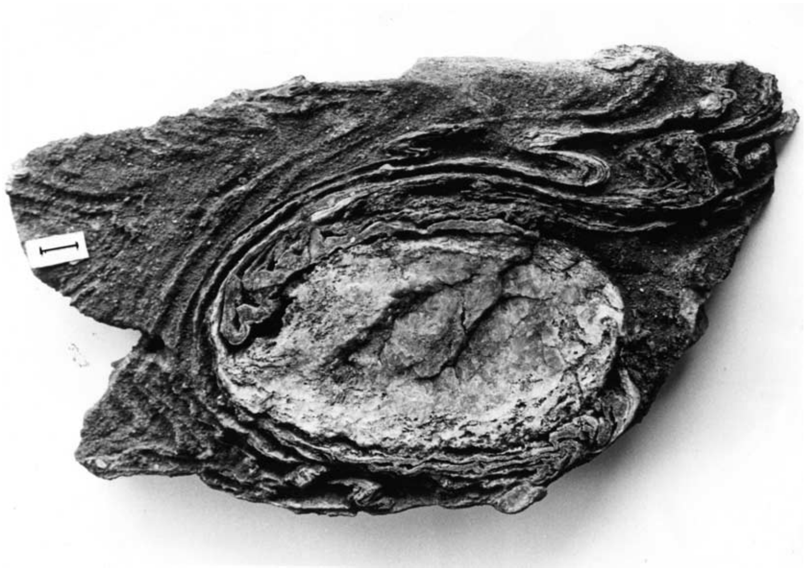

Fig. 13. Horizontal oval section of an elongate pegmatite clast. This section is parallel to E_2 and E_3 of our nomenclature of Fig. 15. The mylonitic foliation in the neighbourhood is asymmetrically deformed with embaying folds forming isoclinal overturned structures suggesting a rotation of 180°. In foliation-parallel sections the long-axis (i.e. E_1 axis) of the cylindrical clast is elongated to at least few tens of decimetres along the down-dip direction of stretching lineation. Scale bar 1 cm.

Brun (1987) and in δ type mantled porphyroclasts. The degree of asymmetry of the rolling structures varies greatly (Fig. 8). On one hand, there are rolling structures around relatively larger quartzofeldspathic clasts indicating rotation through at least 180° (Fig. 13); on the other hand, there are ϕ type porphyroclasts with more or less symmetrical tails, weakly asymmetric σ_a type of porphyroclasts (Passchier and Simpson, 1986) and mantle-free porphyroclasts with symmetrically distorted foliation around them (Fig. 8d).

The asymmetry of rolling structures depends upon several factors (Passchier and Simpson, 1986; Passchier, 1987; Passchier and Trouw, 1996), including the relative rates of deformation and recrystallization and the changing shape of the shrinking clasts. One of the reasons for the wide range of asymmetry of the rolling structures of either the first or the second type, in the same outcrop or in the same thin section, is that different clasts have acquired their present shape and size at different stages of progressive deformation. Moreover, even when a clast retains its shape and size for a long interval of progressive deformation, the asymmetrically deformed mantle or the distorted pattern of foliation around the clast may be destroyed and replaced by a new pattern at a later stage of deformation. In either case, the current pattern of rolling structure would record only a part of the total amount of rotation that the remnant clast has undergone. In the Phulad shear zone, the strongest asymmetry is generally found in the second type of rolling structure around the relatively larger tectonic clasts (in scale of hand specimen), as in Fig. 13, because they retained their size and shape for a relatively longer interval and the coarser scale embaying folds around them were more likely to have survived a large strain during progressive deformation.

6.3. Reorientation of rolling structures around long clasts

In vertical dip-sections of the Phulad shear zone, the asymmetry of rolling structures around clasts consistently indicates a thrusting sense of shear, with clockwise rotation of clasts in NE facing sections and counter-clockwise rotation in SW facing sections (Fig. 14a–d). However, rolling structures associated with strongly rotated clasts frequently appear in horizontal outcrops also (Fig. 14e and f). Thus, for example, Fig. 13 shows the horizontal face of a long cylindrical tectonic clast of pegmatite, with an elliptical cross-section and with the longest axis subparallel to the down-dip stretching lineation. On the horizontal cross-sectional face, the asymmetry of the rolling structure of distorted foliation indicates rotation through an angle of about 180°.

The sense of asymmetry of rolling structures on horizontal outcrops is both dextral and sinistral, although sinistral sense is more common than dextral. The occurrence of such strongly asymmetric rolling structures on a section parallel to the vorticity vector is explained by the model (Ghosh et al., 2003) of rotation of the long axis of a cylindrical clast through a large angle within the foliation plane during progressive transpressional deformation. Let the long axis of a cylindrical clast be designated E_1 and the two axes of the elliptical cross-section be E_2 and E_3, with $E_2 > E_3$ (Fig. 15a). According to this model, the E_1 axis of the clast was initially at a low angle to the subhorizontal vorticity vector (Fig. 15b). The sense of rotation of the clast around it is in agreement with the thrusting sense of shear. With progressive deformation, the E_1 axis rotates away from the vorticity vector and towards the stretching lineation. At an advanced stage of ductile shearing the long axis becomes subparallel to the stretching lineation (Fig. 15c). For a fixed

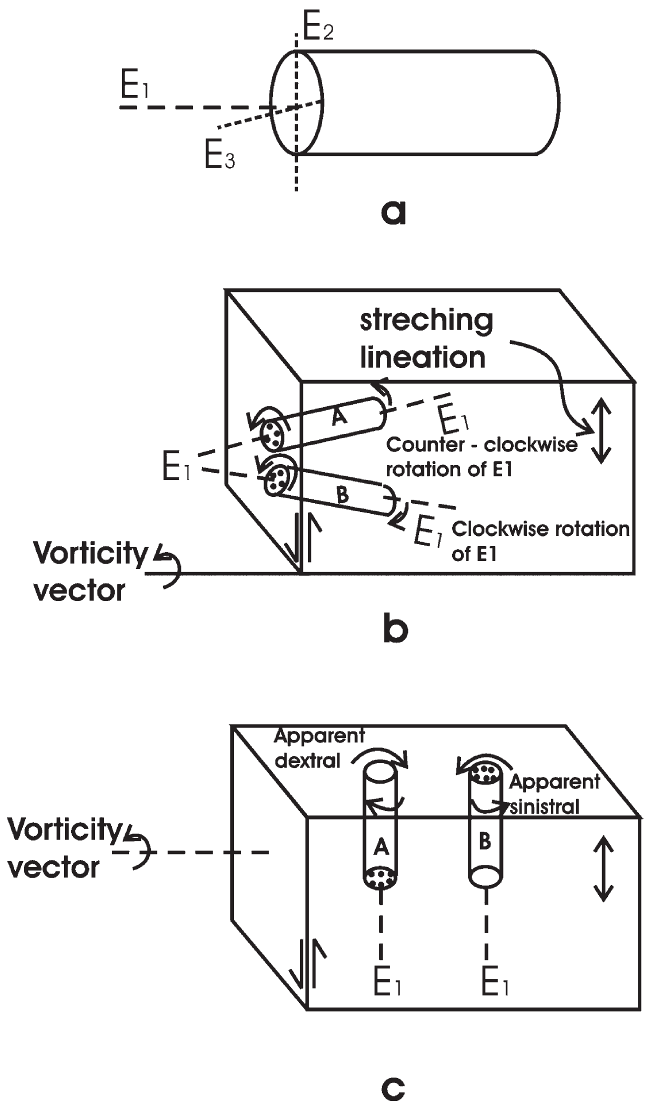

Fig. 15. (a) For a cylindrical tectonic clast, a cylinder axis is designated as E_1. On the elliptic cross-section, two principal axes are designated as E_2 and E_3 with $E_1 > E_2 > E_3$. (b) When E_1 is subhorizontal, the cross-sections of the cylindrical clast rotate counter-clockwise around the E_1 axis on the left hand side of the dip-section in conformity with the vorticity vector. Depending on the initial orientation of E_1, the axis itself rotates on the foliation surface and the cylinder axis will rotate either counter-clockwise (clast A) or clockwise (clast B). (c) On the horizontal surface of the reoriented clast A and B, the sense of rotation would appear to be opposite, apparently dextral in A and apparently sinistral in B.

aspect ratio E_2/E_3, the rate of rotation of E_2 (or E_3) around E_1 is maximum when E_1 is parallel to the vorticity vector; the rate of rotation decreases progressively and tends to become zero as E_1 tends to approach the transport direction. A strongly monoclinic rolling structure is mostly produced during the period when the E_1 axis is at a relatively low angle to the vorticity vector. In accordance with the sense of vorticity, the rotational fabric has a clockwise sense on dip sections while looking towards SW and a counter-clockwise sense on sections while looking towards NE. This asymmetric pattern is retained when the E_1 axis rotates to become subparallel to the stretching lineation. Depending upon the initial orientation of the E_1 axis, its sense of rotation is either in a clockwise or counter-clockwise sense, when looking against the dip direction. Consequently, on the horizontal outcrop face the reoriented rolling structures can show both dextral and sinistral senses of monoclinic symmetry (Fig. 15c).

7. Discussion

Transpressional deformation in a ductile shear zone can be identified from evidence of wall-parallel shearing along with shortening across the shear zone walls. In the course of progressive mylonitization, the original grain size of the shear zone rock is greatly reduced, and strain in the individual grains is associated with recrystallization. Consequently, most major ductile shear zones do not preserve strain markers from which the principal strains can be determined. The transpressional nature of deformation can, however, be qualitatively established from an analysis of the geometry and geometrical evolutions of its structural elements. An approximate idea of the type of transpression (e.g. Fossen and Tikoff, 1998; Ghosh, 2001) can also be obtained from a combined study of a variety of features, e.g. the nature of bulk deformation, orientation of the stretching lineation with respect to the vorticity vector, shear sense indicators, orientations of shear zone cleavage, the geometrical evolution and rotation history of contemporary folds, the patterns of deformed lineations over the folds, pressure shadow around porphyroclasts and the geometry of rolling structures.

As a first approximation, different types of transpressional deformation can be distinguished by using the model of homogeneous transpression with no volume change. In this model of combined simple shearing and three-dimensional pure strain, the direction of simple shearing (with strain rate $\gamma^\bullet$) is parallel to a principal axis of pure strain (with strain rates $\epsilon_x^\bullet$, $\epsilon_y^\bullet$ and $\epsilon_z^\bullet$). The nature of transpression depends largely upon the relative values of a $(= \epsilon_x^\bullet/\gamma^\bullet)$, b $(= \epsilon_y^\bullet/\gamma^\bullet)$ and c $(= \epsilon_z^\bullet/\gamma^\bullet)$. When there is no volume change, the nature of instantaneous deformation can be represented by a point on the ab-plane (Fig. 3).

This analysis shows that it may be possible to identify a broad group of transpressional deformations from a detailed investigation of the geometry of mesoscopic structures and the history of geometrical evolution. The mylonites of the Phulad shear zone show an intense deformation, with a more or less uniform orientation of the foliation parallel to the shear zone boundaries. Deciphering the successive stages of progressive deformation in the Phulad shear zone was facilitated by the occurrence of large tectonic clasts of pegmatite that contain different domains showing deformation ranging from very weak to large. In the high strain Phulad shear zone, evidence of general flattening, evidence of a thrusting sense of shear, occurrence of transport-parallel stretching lineation, frequent occurrence of sheath folds with apical directions parallel to the stretching lineation and occurrence of U-shaped lineation patterns (Ghosh et al., 1999) indicate that the deformation is transpressional, with b/a ranging between -1 and -2.

Since the relatively larger pegmatitic clasts show a newly initiated shear zone foliation at a low angle to the general high strain foliation of the groundmass, we can conclude that the bulk deformation was not dominated by simple shear. This is also confirmed by the presence of symmetrical U-shaped lineations, which develop only when the deformation involves both simple shear and pure strain (Ghosh et al., 1999).

The deformation has caused rotation of rigid clasts through large angles, even up to 180°. Hence, the absolute values of a and b were not very small, and it is likely that both simple shear and coaxial strain rates were significantly large. Moreover, occurrence of strongly rotated fold hinges and of the axes of long tectonic clasts within the foliation surface suggests that $a \gg c > 0$. In other words, the rate of extrusion parallel to the subhorizontal vorticity vector was much smaller than that along the up-dip transport direction.

A consequence of rotation of axes of foliation-parallel, long, tectonic clasts in the Phulad shear zone is that strongly monoclinic rolling structures may be reoriented and may appear in vorticity-parallel horizontal sections. The asymmetry of these rolling structures on the horizontal outcrop face is a feature that was inherited from an earlier stage of rotation of the long tectonic clasts. Their sense of asymmetry on the horizontal surface may be both dextral and sinistral in different domains, although the component of strike-parallel shear on the surface is zero.

Acknowledgements

This work was made possible by the financial support of the Council of Scientific and Industrial Research and the Indian National Science Academy. We thank Santanu Bose for his help in drafting the line drawings. We are grateful to Joao Hippert, Iain Allison and Hemin Koyi for their critical comments and suggestions.

References

Alsop, G.I., 1992. Progressive deformation and the rotation of contemporary fold axes in the Ballybofey Nappe, north-west Ireland. Geological Journal 27, 271–283.

Alsop, G.I., Holdsworth, R.E., 1999. Vergence and facing patterns in large-scale sheath folds. Journal of Structural Geology 21, 1335–1349.

Bell, T.H., 1978. Progressive deformation and reorientation of fold axes in a ductile mylonite zone: the Woodroffe thrust. Tectonophysics 44, 285–320.

Bryant, B., Reed, J.C., 1969. Significance of lineation and minor folds near major thrust faults in the southern Appalachian and the British and Norwegian Caledonides. Geological Magazine 106, 412–429.

Carreras, J., Estrada, A., White, S., 1977. The effect of folding on the c-axis fabric of a quartz mylonite. Tectonophysics 39, 3–24.

Cobbold, P.R., Quinquis, H., 1980. Development of sheath folds in shear regimes. Journal of Structural Geology 2, 119–126.

Crispini, L., Capponi, G., 1997. Quartz fabric and strain partitioning sheath folds: an example from the Voltri Group (Western Alps, Italy). Journal of Structural Geology 19, 1149–1157.

Dutton, B.J., 1997. Finite strain in transpression zones with no boundary-slip. Journal of Structural Geology 19, 1189–1200.

Escher, A., Watterson, J., 1974. Stretching fabrics, folds and crustal shortening. Tectonophysics 22, 223–231.

Fossen, H., Tikoff, B., 1993. The deformation matrix for simultaneous simple shearing, pure shearing and volume change, and its application to transpression-transtension. Journal of Structural Geology 15, 413–422.

Fossen, H., Tikoff, B., 1998. Extended models of transpression and transtension, and application to tectonic settings. In: Holdsworth, R.E., Strachan, R.A., Dewey, J.F. (Eds.), Continental Transpressional and Transtensional Tectonics, Geological Society of London Special Publications, 135., pp. 15–33.

Ghosh, S.K., 1975. Distortion of planar structures around rigid spherical bodies. Tectonophysics 28, 185–208.

Ghosh, S.K., 1977. Drag patterns of planar structures around rigid inclusions. In: Saxena, S.K., Bhattacharji, S. (Eds.), Energetics of Geological Processes, Springer-Verlag, New York, pp. 94–120.

Ghosh, S.K., 2001. Types of transpressional and transtensional deformation. In: Koyi, H.A., Mancktelow, N.S. (Eds.), Tectonic Modeling: A Volume in Honor of Hans Ramberg, Geological Society of America Memoir, 193., pp. 1–20.

Ghosh, S.K., Chatterjee, A., 1985. Patterns of deformed early lineations over late folds formed by buckling and flattening. Journal of Structural Geology 7, 651–666.

Ghosh, S.K., Ramberg, H., 1976. Reorientation of inclusions by combination of pure shear and simple shear. Tectonophysics 34, 1–70.

Ghosh, S.K., Sengupta, S., 1984. Successive development of plane noncylindrical folds in progressive deformation. Journal of Structural Geology 6, 703–709.

Ghosh, S.K., Sengupta, S., 1987. Progressive evolution of structures in a ductile shear zone. Journal of Structural Geology 9, 277–288.

Ghosh, S.K., Sengupta, S., 1990. Singhbhum Shear Zone: structural transition and a kinematic model. Proceedings of the Indian Academy of Sciences (Earth and Planetary Sciences) 99, 229–247.

Ghosh, S.K., Khan, D., Sengupta, S., 1995. Interfering folds in constrictional deformation. Journal of Structural Geology 17, 1361–1373.

Ghosh, S.K., Hazra, S., Sengupta, S., 1999. Planar, non-planar and refolded sheath folds in Phulad shear zone, Rajasthan, India. Journal of Structural Geology 21, 1715–1729.

Ghosh, S.K., Sen, G., Sengupta, S., 2003. Rotation of long tectonic clasts in transpressional shear zones. Journal of Structural Geology 25, 1083–1096.

Greene, D.C., Schweickert, R.A., 1995. The Gem lake shear zone: Cretaceous dextral transpression in the northern Ritter Range pendant, eastern Sierra Nevada, California. Tectonics 14, 945–961.

Hazra, S., 1997. Sense of fold asymmetry in single phase and superposed folding. In: Sengupta, S., (Ed.), Evolution of Geological Structures in Micro- to Macro-scales, Chapman and Hall, pp. 397–409.

Hudleston, P.J., Schultz-Ela, D., Southwick, D.L., 1988. Transpression in Archean Greenstone belt, Minnesota. Canadian Journal of Earth Science 25, 1060–1068.

Jones, R.R., Holdsworth, R.E., 1998. Oblique simple shear in transpression zones. In: Holdsworth, R.E., Strachan, R.A., Dewey, J.F. (Eds.), Continental Transpressional and Transtensional Tectonics, Geological Society, London, Special Publications, 135., pp. 35–40.

Jones, R.R., Holdsworth, R.E., Bailey, W., 1997. Lateral extrusion in transpression zones: the importance of boundary conditions. Journal of Structural Geology 19, 1201–1217.

Mies, J.W., 1991. Planar dispersion of folds in ductile shear zones and kinematic interpretation of fold-hinge girdles. Journal of Structural Geology 13, 281–297.

Minnigh, L.D., 1979. Structural analysis of sheath folds in a meta-chert from the western Italian Alps. Journal of Structural Geology 1, 275–282.

Passchier, C.W., 1987. Stable positions of rigid objects in noncoaxial flow - a study in vorticity analysis. Journal of Structural Geology 9, 679–690.

Passchier, C.W., Simpson, C., 1986. Porphyroclast systems as kinematic indicators. Journal of Structural Geology 8, 831–843.

Passchier, C.W., Trouw, R.A.J., 1996. Microtectonics, Springer, Berlin.

Quinquis, H., Audren, C., Brun, J.P., Cobbold, C., 1978. Intense progressive shear in Ile de Groix blueschists and compatibility with subduction and obduction. Nature 273, 43–45.

Ramberg, H., 1975. Particle paths, displacement and progressive strain applicable to rocks. Tectonophysics 28, 1–37.

Ramsay, J.G., 1967. Folding and Fracturing of Rocks, McGraw-Hill.

Ramsay, J.G., 1980. Shear zone geometry: a review. Journal of Structural Geology 2, 83–99.

Rhodes, S., Gayer, R.A., 1977. Non-cylindrical folds, linear structures in the X direction and mylonite developed during translation of the Caledonian Kalak Nappe Complex of Finnmark. Geological Magazine 114, 329–408.

Robin, P.Y., Cruden, A.R., 1994. Strain and vorticity patterns in ideally ductile transpressional zones. Journal of Structural Geology 16, 447–466.

Sanderson, D.J., 1973. The development of fold axis oblique to the regional trend. Tectonophysics 16, 55–70.

Sanderson, D.J., Marchini, R.D., 1984. Transpression. Journal of Structural Geology 6, 449–458.

Sengupta, S., Ghosh, S.K., 1997. The kinematic history of the Singhbhum Shear Zone. Proceedings of the Indian Academy of Sciences (Earth and Planetary Sciences) 106, 185–196.

Simpson, C., De Paor, D.G., 1993. Strain and kinematic analysis in general shear zones. Journal of Structural Geology 15, 1–20.

Simpson, C., De Paor, D.G., 1997. Practical analysis of general shear zones using the porphyroclast hyperbolic distribution method: an example from the Scandinavian Caledonides. In: Sengupta, S., (Ed.), Evolution of Geological Structures in Micro- to Macro-scales, Chapman and Hall, pp. 169–184.

Tikoff, B., Fossen, H., 1993. Simultaneous pure and simple shear: the unified deformation matrix. Tectonophysics 217, 267–283.

Tikoff, B., Greene, D., 1997. Stretching lineations in transpressional shear zones: an example from the Sierra Nevada Batholiths, California. Journal of Structural Geology 19, 29–39.

Van Den Driessche, J., Brun, J.-P., 1987. Rolling structures at large shear strains. Journal of Structural Geology 9, 691–704.